The Macrophage Proteome Defines the Long Acting Antiretroviral Therapy Cell Depot

Dongwei Guo *, Mariluz Araínga *, Jayme Horning, Pawel Ciborowski, Xin-Ming Liu, JoEllyn McMillan, Howard E. Gendelman
***First two authors contributed equally**
University of Nebraska Medical Center, Omaha, NE

UNIVERSITY OF NEBRASKA MEDICAL CENTER

Dongwei Guo
Department of Pharmacology and Experimental Neuroscience
985800 Nebraska Medical Center
Omaha, NE 68198-5800
Phone: 1-402-559-4044
Fax: 1-402-559-7495
Email: dongwe.guo@unmc.edu

University of Nebraska Medical Center

Introduction

Long acting nanoformulated antiretroviral therapy (nanoART) is emerging as an important part of the treatment armamentarium for human immunodeficiency virus type one (HIV-1) infection. While our prior studies defined both a platform for drug delivery and the trafficking mechanisms operative for nanoART in monocyte-macrophages, how these cells can be harnessed as drug depots for improved antiretroviral responses has not been realized. Indeed, human monocyte-derived macrophages (MDM) serve as nanoART carriers extending ART half-life and drug stability. Such cell-based drug delivery strategies may also decrease systemic drug toxicities. We posit that endolysosomal pathways can serve as Trojan horses for viral persistence or as vehicles for its elimination. If correct, facilitated viral replication and the means to eliminate it may occur at identical subcellular locales. The operative nanoART response would facilitate drug delivery by bringing the medicine to the site of action within mononuclear phagocytes (MP; monocytes, macrophages and dendritic cells). To investigate a seemingly mechanistic paradox, functional proteomic tests were employed to uncover how drug particles affect the HIV-1 replication cycle beyond nanoART activity.

Methods

Nanoformulated P407-ATV (nanoATV) was prepared by high-pressure homogenization using an Avestin Emulsiflex C3 homogenizer. Human peripheral blood monocytes from four donors were cultivated for seven days before 4 hours HIV-1 infection, and then 100 μM nanoATV was treated for 16 hours. Monocyte-derived macrophage (MDM) samples were collected seven days after treatment, and we applied quantitative SWATH-MS proteomic and cell profiling to MDM. DAVID and KEGG bioinformatics tools were used to define the mechanistic pathways that facilitate cell-nanoATV carriage while limiting viral growth. HIV-1 reverse transcriptase (RT) activity was measured to assess antiretroviral efficacy in HIV-1 infected MDM. Protein expressions of Rab 5, 7 and 11, LAMP-1 and Actin were detected by Western blot assays.

Results

Both HIV-1 and nanoATV engaged phagolysosomal trafficking pathways. However, MDM phagolysosomal proteins were deregulated in opposing directions. Paired-samples Z-test showed that an up-regulation of phagolysosomal proteins by HIV-1 was reversed by nanoATV. DAVID and KEGG bioinformatics tools defined the signaling pathways for cell-nanoATV carriage that may limit viral growth. These phagolysosomal protein sets were linked to macrophage functions that included phagocytosis, antigen presentation, secretory activities, phagocytic and cell migration responses. KEGG pathway analyses indicated phagosome signalling as one of the main pathways related to HIV infection and nanoATV treatment. KEGG revealed the up-regulation of Rab5 and -7 proteins in HIV-1 infected cells; in contrast these same proteins were down-regulated in nanoATV-treated HIV-infected cells. Western blot results showed a clear down regulation in the expression of Rab5, -7, -11 and LAMP1 proteins after nanoATV treatment. Measures of HIV reverse transcriptase activity in infected cells treated with nanoATV showed attenuation of viral infection. Cytokine assays demonstrated that IL12 and TNF were increased in HIV-1 infected macrophages but reduced with nanoATV treatment.

Conclusions

HIV-1 and nanoATV deregulate cellular proteins in opposing manners. The common pathways are linked to viral assembly and are endolysosomal-linked. Rab5, -7, -11 and LAMP1 serve to coordinate molecular and biological functions of the virus and the antivirus in subcellular compartments. Alterations made by HIV-1 and nanoATV indicate that specific organelles are action sites for both. These findings provide novel insights into the role played by long acting subcellular targeted nanotherapies for combatting HIV-1 infection.

References

1. Boffito M, Jackson A, Owen A, Becker S: New approaches to antiretroviral drug delivery: challenges and opportunities associated with the use of long-acting injectable agents. Drugs 2014, 74:7-13.
2. Gendelman HE, Gelbard HA: Adjunctive and long-acting nanoformulated antiretroviral therapies for HIV-associated neurocognitive disorders. Curr Opin HIV AIDS 2014, 9:585-590.
3. Guo D, Zhang G, Wysocki TA, Wysocki BJ, Gelbard HA, Liu XM, McMillan JM, Gendelman HE: Endosomal trafficking of nanoformulated antiretroviral therapy facilitates drug particle carriage and HIV clearance. J Virol 2014, 88:9504-9513.
4. Kadiu I, Nowacek A, McMillan J, Gendelman HE: Macrophage endocytic trafficking of antiretroviral nanoparticles. Nanomedicine (Lond) 2011, 6:975-994.

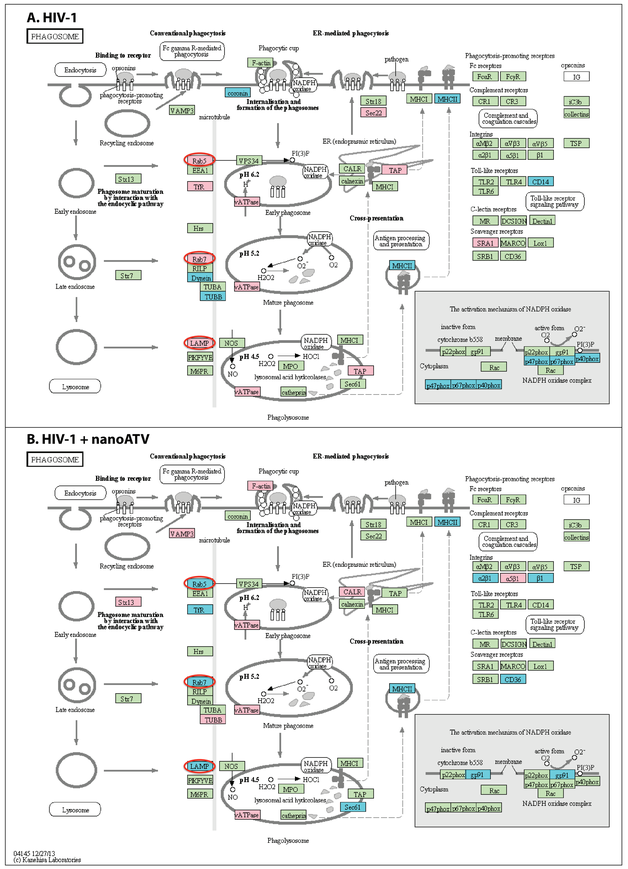


Figure 1. Schematic representation of the MDM phagosome network identified in HIV-1-infected (A) and HIV-1-infected and nanoATV treated cells (B). Proteins identified were compared against control uninfected MDM cultures ($p<0.05$). The acquired protein expression profiles were analyzed using a comprehensive set of functional annotation tools to uncover biological data sets behind the uncovered list of genes. Data for Annotation, Visualization and Integrated Discovery (DAVID) analysis was employed to identify enriched biological processes among the expressed proteins. Gene Ontology terms were used to identify related pathways with the assistance of the Kyoto Encyclopedia of Genes and Genomes (KEGG) database. The KEGG database facilitated the elucidation of the level functions for the MDM as derived from the proteomic datasets. Statistical significance was determined using a p-value < 0.05. Proteins in red and blue, display up- and down- regulation, respectively. Proteins in green belong to the phagosome network and not deregulated by ATV treatment.

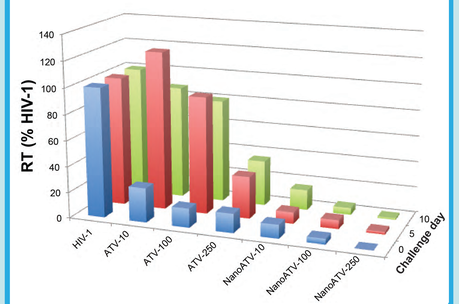


Figure 2. NanoATV treatment effects HIV-1 reverse transcriptase (RT) activity. HIV-1 RT activity was determined in treated (native ATV or nanoATV) MDM followed by HIV-1 infection at days 0, 5 or 10. HIV-1 infected cells, without any treatment, served as a positive control for RT activity. All samples were collected after 7 days of viral infection. Results shown are the mean of 5 replicates.

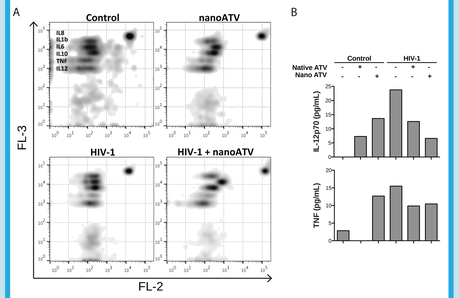
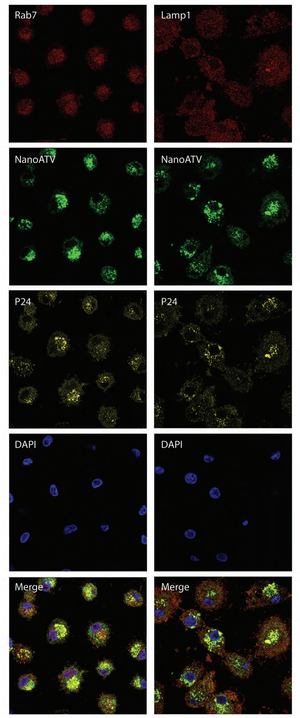


Figure 5. NanoATV regulation of cytokine profiles in HIV-1 infected MDM. MDM were treated with 100 μM native ATV or nanoATV and infected with HIV-1 at day 0, 5 or 10 post-drug treatment. Untreated, uninfected cells were used as controls. After 24 hours of viral infection, cell culture media were collected and analyzed using a cytokine bead array. (A) Density plots show expression of IL-12, TNF, IL-10, IL-6, IL-1β and IL-8 for control, treated, HIV-1 infected and treated infected MDM. Cytokine levels were detected by FACSArray cytometer and data was plotted using FlowJo (version 10.7) software. (B) Levels of IL-12 and TNF after treatment and infection are shown. Data are analyzed using FCAP software and values of cytokine expression were expressed as pg/mL.



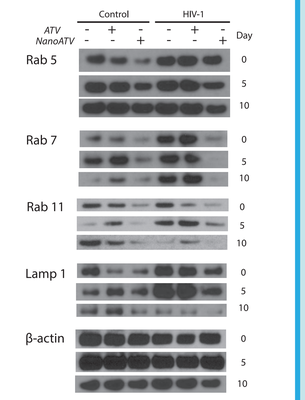


Figure 3. NanoATV and HIV-1 endosomal protein regulation. Western blot of Rab5, -7, -11, LAMP1 and β-actin was performed in cell lysates from MDM treated with native ATV or nanoATV and infected with HIV-1 at day 0, 5 or 10 post-drug treatment then incubated for 7 days.

Figure 4. Subcellular localization of nanoATV, HIV-1 and endolysosomal proteins. Cellular localization of Rab7 or LAMP1 endosomal compartments (red), HIV-1p24 (yellow) and nanoATV (green) are shown by confocal microscopy. Cell nuclei were stained with DAPI (blue). Merged images showed the co-localization of all proteins.

Table 1. Endolysosomal proteins in HIV-1, HIV+nanoATV, nanoATV and native ATV treated MDM.

		HIV		*HIV+nanoATV*		*nativeATV*		*nanoATV*	
	Protein	Ztest	Regulation	Ztest	Regulation	Z test	Regulation	Z test	Regulation
Early endosomes	Rab5	4.09	↑	-2.57	↓	-2.35	↓	2.87	↑
	TAP	3.38	↑	--	↔	--	↔	--	↔
	TfR	2.62	↑	-3.02	↓	--	↔	--	↔
	vATPase	3.70	↑	2.32	↑	-5.21	↓	-2.02	↓
	Stx13	--	↔	3.47	↑	--	↔	-2.43	↓
	EEA1	--	↔	--	↔	2.62	↑	--	↔
	VPS34	--	↔	--	↔	--	↔	--	↔
	CALR	--	↔	2.03	↑	2.29	↑	-3.73	↓
	Calnexin	--	↔	--	↔	-3.40	↔	--	↔
Late endosomes	Rab7	2.71	↑	-2.62	↓	3.87	↑	--	↔
	vATPase	3.70	↑	2.30	↑	-5.20	↓	-2.02	↓
	Dynein	-2.01	↓	--	↔	--	↔	--	↔
	TUBB	-2.90	↓	2.81	↑	--	↔	--	↔
	TUBA	--	↔	--	↔	--	↔	--	↔
	RILP	--	↔	--	↔	--	↔	--	↔
	Stx7	--	↔	--	↔	--	↔	--	↔
Lysosomes	LAMP	2.88	↑	-2.23	↓	--	↔	--	↔
	vATPase	3.70	↑	2.30	↑	-5.20	↓	-2.02	↓
	TAP	3.40	↑	--	↔	--	↔	--	↔
	M6PR	--	↔	--	↔	--	↔	--	↔
	Cathepsin	--	↔	--	↔	--	↔	--	↔

↓ *Downregulated* ↔ *Unchanged* ↑ *Upregulated*